

Review

Interfacial Flows and Interfacial Shape Modulation Controlled by the Thermal Action of Light Energy

Natalia Ivanova ^{1,2} 

¹ Photonics and Microfluidics Laboratory, X-BIO Institute, University of Tyumen, 6 Volodarskogo, 625003 Tyumen, Russia; n.a.ivanova@utmn.ru

² Microfiltration Processes Laboratory, WCRC “Advanced Digital Technologies” University of Tyumen, 6 Volodarskogo, 625003 Tyumen, Russia

Abstract: The review covers the research on thermocapillary convection caused by the thermal action of laser radiation in single-layer and bilayer liquid systems of capillary thickness. The advantages of using optical radiation are the instantaneous delivery of thermal energy to a place on demand (a bulk phase, interfaces); low radiation power required; concentrating heat flux on a spot of a few micrometers; the production of arbitrary spatial distributions of radiation intensity; and, as a result, corresponding thermal fields at a liquid interface and their fast reconfiguration. Thermocapillary stresses at the liquid interfaces lead to the transfer of the liquid and a change in the shape of the interface, in accordance with the distribution of the light-induced thermal field. Studies concerned with the methods of non-destructive testing of liquid media and solids, which are based on a photothermocapillary signal emitted by a laser-induced concave deformation of a thin layer, are considered. Features of thermocapillary deformation of a liquid–air interface caused by local heating of thin and thick (exceeding the capillary length) layers are demonstrated. A part of the review addresses the results of the study of thermocapillary rupture of films in the heating zone and the application of this effect in semiconductor electronics and high-resolution lithography. The works on the light-induced thermocapillary effect in bilayer (multilayer) liquid systems are analyzed, including early works on image recording liquid layer systems, liquid IR transducers, and nonlinear optical media.

Keywords: light energy; laser induced thermocapillary flow; Marangoni effect; laser induced surface deformation; thin liquid films; surfactant monolayers; photothermal effects



Citation: Ivanova, N. Interfacial Flows and Interfacial Shape Modulation Controlled by the Thermal Action of Light Energy. *Colloids Interfaces* **2022**, *6*, 31. <https://doi.org/10.3390/colloids6020031>

Academic Editors: Victor Starov and Alexander Kamyshny

Received: 14 April 2022

Accepted: 11 May 2022

Published: 13 May 2022

Publisher’s Note: MDPI stays neutral with regard to jurisdictional claims in published maps and institutional affiliations.



Copyright: © 2022 by the author. Licensee MDPI, Basel, Switzerland. This article is an open access article distributed under the terms and conditions of the Creative Commons Attribution (CC BY) license (<https://creativecommons.org/licenses/by/4.0/>).

1. Introduction

Today, optical radiation (light) is widely used as a high-precision and efficient tool for controlling the fluid flow, the shape of the liquid–liquid or liquid–air interfaces, and manipulating small objects suspended in the bulk liquid phase or located on the interfaces. Using light makes it possible to solve a wide range of problems in various applications, including biological research [1–4], liquid diagnostics [5–15], non-destructive evaluation of solids [16–20], methods for studying properties of soft interfaces [21–24], electronic industry [25–31], technologies of tunable and biomimetic optics [8,32–34], image recording systems [35–38], and non-linear optics [39,40].

The advantages of optical radiation as a tool are the non-contact and remote action on the system, the generation of the required spatial and temporal distribution of the light intensity, the tightening focusing and strong localization of the radiation energy, the generation of monochrome, coherent and polarized radiation, the wide range of wavelengths from 10 nanometers to 1 mm; and the large variety of light sources, including sunlight. According to the nature of the action of optical radiation on matter, two ways of converting radiation energy into the kinetic energy of motion can be identified, e.g., in Figure 1. One of them is the direct transfer of the momentum of the light incident on the interface, appearing

as the light pressure or the action of gradient optical forces caused by the refraction and scattering of light at an interface (e.g., a particle-liquid interface). This effect results in the deformation of flexible interfaces or motion of objects suspended in a fluid phase (Figure 1). Another way relies on the absorption of optical radiation by atoms or molecules of liquid medium. In the majority of cases, the effects caused by absorption dominate over the light pressure. The absorption of optical radiation leads to an increase in the internal energy of the absorption centers and their transition to an excited state (the process of photoexcitation). The relaxation of the excited state occurs by converting the absorbed energy through various degradation routes depending on specific conditions. For some media, the energy of the excited state of the absorption centers is converted through photochemical reactions. An example is the reaction of photoisomerization of photosensitive surfactant molecules (see below). Thermal non-radiative relaxation leads to the release of energy in the form of heat and, as a result, to a local increase in the temperature of the liquid medium. In turn, a change in temperature leads to a change in the temperature-dependent physical properties of the liquid.

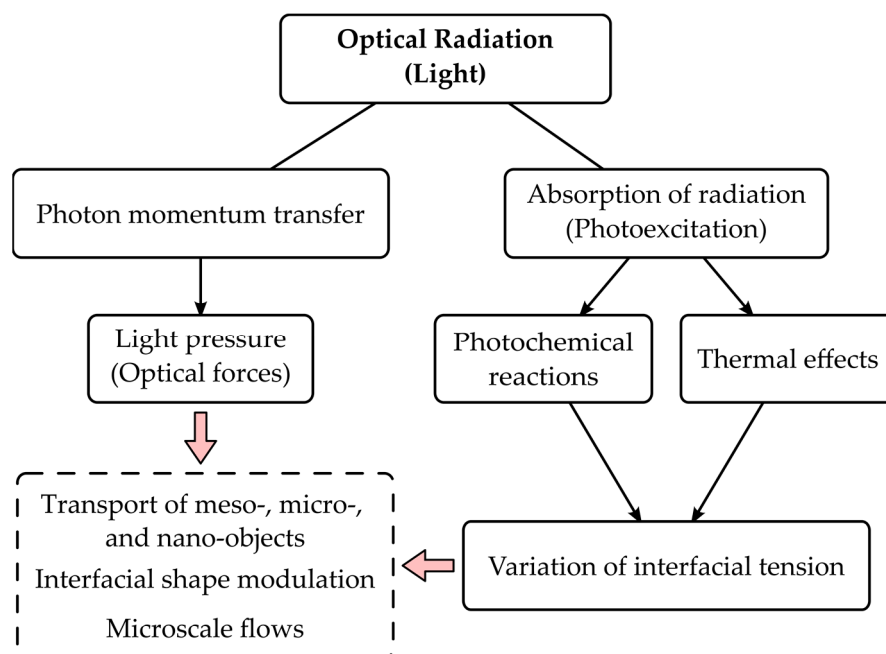


Figure 1. The ways of light energy conversion into kinetic energy of motion.

As is known, the interfacial tension between two fluid phases is sensitive to perturbations of scalar fields of temperature or concentration of components at the interface [41]. These perturbations create the interfacial tension gradient, which due to viscous stress in the bulk phase, ultimately lead to the transport of the liquid [41]. The flow of a liquid medium caused by temperature or concentration gradients is known as the Marangoni effect [42]. The Marangoni flow is directed towards the area of higher interfacial tension. For most pure liquids, the interfacial tension at the liquid–air interface decreases linearly with increasing temperature, although for some liquids that dependence is non-linear over a wide range of temperatures and even shows two opposite trends [43,44].

The nature of the interfacial tension changing due to variation in concentration of admixture strongly depends on the nature of the admixture [45]. For instance, the addition of salts to water leads to a linear increase in the interfacial tension, and surfactants, on the contrary, reduce the interfacial tension, showing a non-linear character. In a number of works, the change in concentration of a volatile admixture in liquid solutions was induced by the thermal effect of optical radiation due to controlled mass transfer across the interface, i.e., by evaporation [46–48]. There is a class of photosensitive, azobenzene-containing surfactants, that change the interfacial tension of liquid due to a reversible change in

the structure of molecules between trans- and cis- forms upon absorption of radiation of different wavelengths (the photoisomerization reaction). A detailed description of this effect and practical applications can be found in the works [49–51].

Note that light pressure does not lead to a variation in the interfacial tension, but the latter is a crucial parameter for effective control of the surface shape using this mechanism. For more information, see works [3,52].

The present review focuses mainly on experimental studies on the thermal Marangoni mechanism of liquid motion, also known as the thermocapillary effect, controlled by the thermal action of optical radiation. The main requirement for optical radiation, regardless of the type of its source, is the absorption of radiation by the medium and its subsequent heating. In other words, the generation of local disturbances in temperature results in thermal gradients on the interfaces. In most of the work, as sources of optical radiation, lasers are used. Lasers generate optical radiation (laser radiation) of high directivity and at a given wavelength. Thermal sources of optical radiation, such as filament lamps and mercury lamps, are also used. However, such sources require the use of a focusing system of lenses and mirrors, and may require the use of monochromators to select a wavelength from their wide spectrum. Thus, the use of lasers is most preferable and effective compared to other sources.

2. Laser-Controlled the Liquid–Air Interfaces and Microscale Flows

The study of the thermal action of laser radiation on thin films and layers of pure non-volatile liquids of a thickness $h_l \leq L_c$ is of great fundamental [53–60] and applied importance [5–33]. Here, $L_c = \sqrt{\gamma_l/\rho_l g}$ is the capillary scale, which is obtained from a balance of the gravity and surface tension forces, the Bond number $Bo \cong 1$.

The heating of a liquid layer with a laser beam (typically with a Gaussian distribution of intensity, $I(r) = \frac{2P}{\pi w_0^2} \exp\left(-\frac{2r^2}{w_0^2}\right)$, across the beam waist, $2w_0$), or any point light source, induces an axisymmetric thermocapillary flow, which transferring the liquid towards the cold area with higher interfacial tension. As a result, a concave deflection of the interface occurs in the local heating area, known as the thermocapillary deflection or cavity, Figure 2a. The pressure underneath the curved interface becomes negative and, consequently, causes the reverse flows towards the heated area near the substrate, which joins outwards thermocapillary flows creating the convective vortex.

In turn, the temperature gradient along the interface can be produced either by the absorption of radiation in the liquid layer itself, according to the Beer–Lambert law, or by the substrate. In the second case, the liquid is optically transparent (non-absorbing); the laser beam passes through the liquid layer and is absorbed by the substrate. As a result, the temperature of the substrate rises in the area of the laser beam incident. The thermal front (an actuating isotherm, ΔT), due to conductive heat transfer from the substrate through the liquid layer, reaches the liquid–air interface and locally increases the interfacial temperature, ΔT . When heating via the substrate, there is a time delay in the start of the thermocapillary flow at the liquid–air interface, which varies with the layer thickness (h_l) and the thermal diffusivity of liquid (χ_l) as $\tau_d \approx h_l^2/\chi_l$.

In the paragraphs below, some peculiarities and practical applications of the thermocapillary convection induced by the thermal action of the laser beam in a liquid layer are considered.

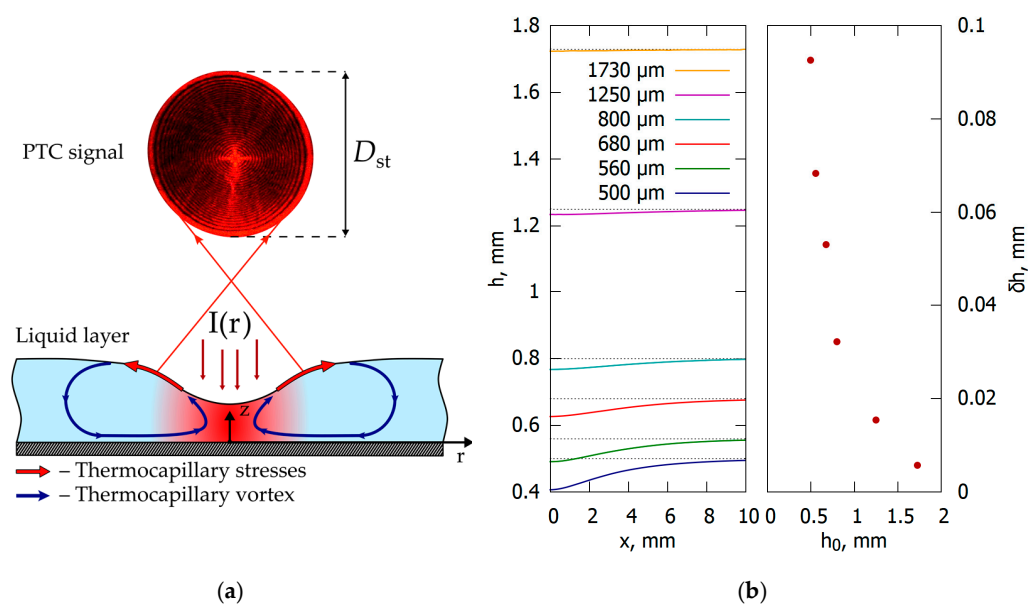


Figure 2. (a) Schematic of the thermocapillary convection in a liquid layer locally heated with a laser beam, $I(r)$. A thermocapillary concave deformation of the interface in the heated spot and the photothermocapillary signal (PTC signal) formation by a reflected laser radiation; (b) typical profiles of the thermocapillary concave deformation of silicone oil layers (500–1730 μm) induced by heating with the laser beam ($\lambda = 532 \text{ nm}$, $P = 12.7 \text{ mW}$) and the deformation depth, δh , vs. the layer thicknesses.

2.1. Photothermocapillary Spectroscopy and Non-Destructive Testing

A distinctive of that laser-induced effect is the fact that the thermocapillary cavity in the liquid layer represents a concave mirror, which partially reflects the incident laser beam. The reflected radiation of the laser beam forms an interference ring pattern on the remote screen called the photothermocapillary response or signal (the PTC signal for short), Figure 2a. A detailed optical scheme explaining the formation of an interference pattern by a reflection from a concave thermocapillary mirror rays is presented in [5]. The structure of the interference ring pattern (the PTC signal) and its diameter, including evolution, both contain information on the properties and parameters of the liquid and the underlying substrate.

A number of studies [5–9] were dealing with the thermocapillary convection in the layers of the heavy oil that strongly absorbs the laser radiation of the visible range. The authors attempted to estimate the shape of the thermocapillary cavity and relate it to the intensity distribution over the laser beam cross section [7,8]. They noted for the first time that thermophysical, rheological and optical properties of a liquid could be determined through analysis of the interference pattern structure [6–9].

Later on, a research group [10–20] developed a new direction in photothermal spectroscopy of liquids [10–15] and non-destructive testing of solids [16–20] based on the effect of the laser-induced thermocapillary convection in thin liquid layers. Low volatile liquids (aromatic hydrocarbons, aromatic alcohols, silicone oils of different viscosity) on absorbing the laser beam ($\lambda = 633 \text{ nm}$, $P \leq 20 \text{ mW}$) substrates were used in experiments. The researchers found out that the stationary diameter of the circle PTC signal (D_{st}), Figure 2a, generated by the steady state thermocapillary cavity of the layer, depends on a number of parameters and properties of the liquid/substrate/laser beam system,

$$D_{st} = f(\gamma, \gamma', \beta, \mu, \rho_i, k_i, \chi_i, h_i, \alpha_i(\lambda), I(r), P). \quad (1)$$

Here, i is a subscript denoting a liquid, $i = l$, or a solid, $i = s$; γ and γ' are the interfacial (surface) tension and the temperature coefficient of the interfacial tension, β is the

volumetric thermal expansion coefficient of liquid, ρ is the density, k is the thermal conductivity, χ is the thermal diffusivity, h is the thickness, $\alpha(\lambda)$ is the light absorption coefficient, λ is the wavelength of radiation, $I(r)$ is the intensity distribution of the laser beam, P is the power of the laser beam. This highly sophisticated functional relationship can be simplified by defining all but one of the parameters, then getting the calibration dependence of D_{st} on that parameter. Based on this approach, non-contact photothermocapillary methods for determining the thickness of transparent liquid layers on flat substrates [10], the viscosity of liquids [11], advancing and receding contact angles of liquids on solid surfaces [12] were developed. Note that, according to experimental data obtained for a number of liquids (octane, o-xylene, butanol, benzyl alcohol) on a light-absorbing carbolite substrate at $P = 5.5$ mW the PTC diameter and the layer thickness are related by the power law,

$$D_{st} \sim h_l^{-n} \quad (2)$$

where n is the power exponent decreasing with viscosity of these liquids. In [13,14], a lag time between the moment of the laser beam turning on and appearance of the PTC signal on a screen was detected. The quadratic dependence of the lag time on the thickness of liquid layer, $\tau_d \approx h_l^2 / \chi_l$ was considered as a basis for a method of measuring the thermal diffusivity of non-absorbing irradiation pure liquids [13]. Later, it was revealed a high-sensitivity of thermocapillary stresses on a free liquid surface to thermal properties of solids that became a basis of photothermocapillary approach to the non-destructive evaluation control of solid samples [16–20]. In this case, the liquid–air interface serves as actuator medium. Basing on analysis of the stationary PTC signal a number of methods to detect in solid samples of different hidden flaws, including caverns and foreign inclusions under varnish and paint coatings [16–18], as well as the quality control of conductive tracks of printed circuit boards were developed [19]. In [20], it was experimentally found that diameter of the PTC signal depends on thermal conductivity of solid materials as

$$D_{st} \sim k_s^{-m} \quad (3)$$

for k_s ranged from 0.1 to 100 W/(m × K), where m is the power exponent, which varies in the range 0.672–0.899 depending on the layer thickness and the power of the laser beam [20].

2.2. Interfacial Shape Exposed to the Light-Induced Thermocapillary Stresses

In some works [32,33], the laser-induced thermocapillary deflection created in thin layers and sessile droplets (volume ≤ 1 μ L) were studied as an adaptive mirror [32] and a tunable converging/diverging lens [33], respectively. It is shown [32] that the focal length, which is inversely related to the curvature of the central part of the thermocapillary deflection, decreases with a decrease in the layer thickness and with an increase in the laser beam power ($F \sim 1/P$). These results indirectly indicate an increase in the slope angle of the interface and the deflection depth due to the intensification of the thermocapillary convection in a layer.

In [61], the shape of the thermocapillary deflection of thin layers of silicone oil (5 cSt) upon the thermal action of the Gaussian laser beam ($\lambda = 532$ nm, $P = 12.7$ mW, $2w_0 = 0.8$ mm) absorbed by the substrate (ebonite) was studied experimentally and numerically. The shape of the steady state thermocapillary deflection was measured by the scanning with a laser knife and then experimental data, Figure 2b, were compared to the numerically obtained shapes [61]. It was shown that the depth of the central part of deflection increases with the decrease in the layer thickness (Figure 2b) that in line with the indirectly obtained results in [32]. Similar tendency was detected in work [62] for the layers (228–550 μ m) of silicone oils in wide range of viscosities from 5 to 400 cSt when irradiating the light-absorbing substrate with the laser beam ($\lambda = 655$ nm, $P = 16.5$ mW). The authors used the laser scanning confocal microscope to measure the deflection depth [62].

It is important to note that in some works [58,63], the light-induced thermocapillary convection and deformation of the liquid–air interface were studied in thick layers, $h_l > L_c$. For example, in [58] the thermocapillary convection was excited in a water layer of 30 mm thick by the CO₂ laser beam ($\lambda = 10.6 \mu\text{m}$, P ranging between 0.6–6 W), and in [63]—in decane layers of 1–10 mm thick, focusing radiation of a filament lamp (1.2–3 W) into the depth of the layer.

An interesting result was that in the area of a locally increasing the interfacial temperature of a thick layer, a convex deformation of the interface is formed, i.e., the interface rises up. In the case of decane [63], the convex shape was detected in the layers at $h_l > 1 \text{ mm}$, and then, when $h_l \leq 1 \text{ mm}$ the interface took on the typical concave shape.

2.3. Light-Induced Rupture of Thin Films and the Control of the Contact Line Instability

A weak side of the laser-induced thermocapillary concave deflection of a liquid layer on a solid surface is the instability of the layer in that area to a rupture. Generally, the instability of thin films and the formation of ruptures and dry out spots in the areas of temperature perturbations is very relevant to the problem for improving the reliability of thin-film cooling systems [64–68] and other thin film applications [67,68]. On the other hand, the control of the rupture process and the formation of a clean non-wetted the rupture area is extremely important for solving problems in immersion lithography—technology for integrated circuits fabrication [69,70].

The studies [25,26] were devoted to the numerical and experimental investigation of the thermocapillary rupture of thin ($h_l \approx 5 \mu\text{m}$) liquid films with a focused IR laser beam ($\lambda = 1470 \text{ nm}$, $2w_0 = 200 \mu\text{m}$) on stationary [25] and rotating substrates [26]. The authors showed that the narrower the beam and the higher the power, the faster the film rupture occurs. In addition, they determined the range of beam powers and substrate rotation speed in which the thermocapillary film rupture and the subsequent dewetting process occur without residual droplets. In [27] the thermal action of the IR laser beam on the receding contact line of a droplet, which represents a liquid bridge between the needle tip and the rotating substrate, was studied. It was shown that the generation of the thermocapillary flows on the receding part of the droplet leads to an increase in the mobility of the contact line, prevents fragmentation and formation of residual droplets. Finally, it makes it possible to increase the substrate rotation speed that is crucially important for improving the quality and throughput of fabrication in large-scale electronics by immersion lithography.

Feasibility of applying the optical radiation to suppress the fingering instability along a contact line of a thin film of low-viscous silicone oil (0.65 cSt) spreading on a substrate was shown in [71]. As a source of radiation, the authors used the spatial and temporal modulated radiation of an arc lamp, which was absorbed by the substrate creating a thermal field along the fingering front. As a result, the thermocapillary flow from the irradiated (heated) areas towards the non-irradiated areas appeared, thus leveling disturbances of the spreading front. The use of feedback and the fast rearrangement of the spatial distribution of light intensity allows for an effective tool for monitoring and studying instabilities [71].

The study [28,29] demonstrated the rupture of hexadecane layer ($\sim 1 \text{ mm}$ thick) on light-absorbing substrates induced by a laser knife ($\lambda = 1.5 \mu\text{m}$, length of the beam $\sim 1 \text{ cm}$, $P = 500 \text{ mW}$) and subsequent transfer of liquid (i.e., receding of the three-phase contact line) in front of slow displacing laser line along the substrate, Figure 3a. This mechanism was shown to be effective for cleaning the surfaces from particulate impurities. Micro- and nanoparticles adherent to substrate were removed by the laser-induced thermocapillary flow.

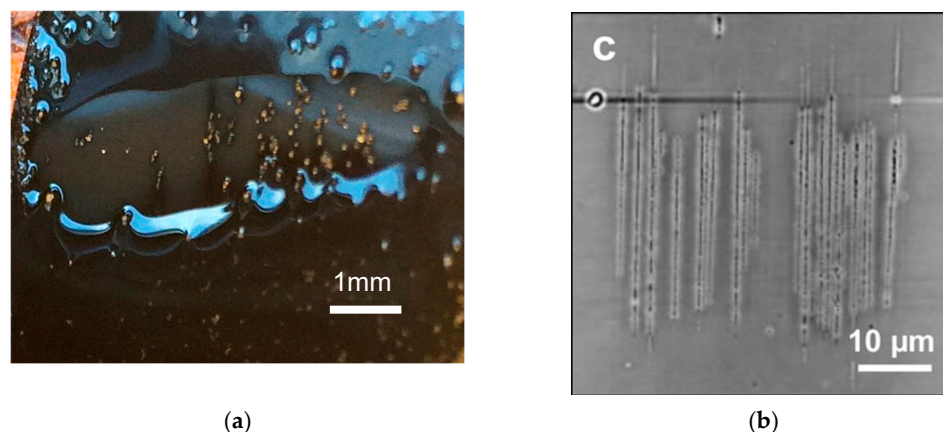


Figure 3. Top view images of the laser-induced thermocapillary ruptures: (a) the rupture of hexadecane layer (~ 1 mm thick) on a wetted soft magnetic disc caused by a line beam of IR laser. Residual polyethylene particles are captured by receding three phase contact line in the rupture area; (b) selective trench formation in the thermocapillary resist layer caused by laser exposure [30]. Trenches of ~ 20 nm in the depth, ~ 100 nm in the width and around $60 \mu\text{m}$ length. Reprinted with permission from ACS Nano, 2014, 8, 12641. Copyright 2022 American Chemical Society.

The formation of the thermocapillary trenches of 100 nm width in the areas of selective absorption of the IR radiation of the scanning laser ($\lambda = 2500$ nm, $5 \mu\text{m}$ spot diam.) by metallic single-walled carbon nanotubes (metallic-SWNTs) grown on a glass surface allows them to be effectively deleted by the reactive electron etching [30], Figure 3b. Meanwhile, useful non-absorptive semiconducting-SWNTs are saved under the protective liquid layer 25 nm thick [30]. This approach solves the problem of improving the quality of transistors and semiconductor electronics [30].

A laser-direct write of positive tone as the high resolution and low power alternative for lithographic techniques utilizing the effect of thermocapillary dewetting (in other words the thermocapillary ruptures) was proposed in [31]. By scanning of a thin film of polystyrene (50–60 nm thick) on a silicone substrate with a laser beam ($\lambda = 532$ nm, 232–240 mW at scanning rate $100 \mu\text{m/s}$) it was possible to create the array of lines with resolution better than $1 \mu\text{m}$. Due to the thermocapillary flows, liquid spread out from the moving laser spot, resulting in a long trench similarly to that found in work [31]. Thus, in the irradiated area the silicone substrate became free from the coating material.

The study [72] demonstrates for the first time the possibility of generating thermocapillary flows at the liquid-substrate interface by the thermal action of a laser beam. The authors prepared a superhydrophobic substrate to enable the Cassie wetting condition with the water layer when that substrate covers the layer from above. A tiny air gap ($30 \mu\text{m}$ thick) between the substrate and water layer, which was filled with a hydrophobized structure of the light-absorbing soot on the substrate, served as a driving interfaces. The thermal gradient was produced by an irradiating the substrate with the laser beam ($\lambda = 488$ nm, spot size $350 \mu\text{m}$, $P = 10$ mW), and minimal thermal gradient of 0.2 K/cm was enough to generate the thermocapillary liquid flow [72].

2.4. Laser-Induced Marangoni Flows on the Liquid-Surfactant Interfaces

The effect of surfactant additives to pure liquid on the thermally induced Marangoni convection opens up the perspectives for the development of highly sensitive instruments for physicochemical analysis [14], the study of the surfactant films rheology [21,22,73] and solving problems in microfluidics [23,24].

The main feature of such convection is the competition between two mechanisms of opposite action. The thermocapillary mechanism of the transfer of surfactant molecules along the interface away from the heating spot resulting in a compressed layer of surfactant molecules on the periphery. This led to a decrease in the interfacial tension at the periphery,

and therefore, to appearing a stronger opposite interfacial tension gradient, called the concentration Marangoni effect. As a result, the flow changes its direction towards the heated area and lead to suppression of the thermocapillary effect (Figure 4).

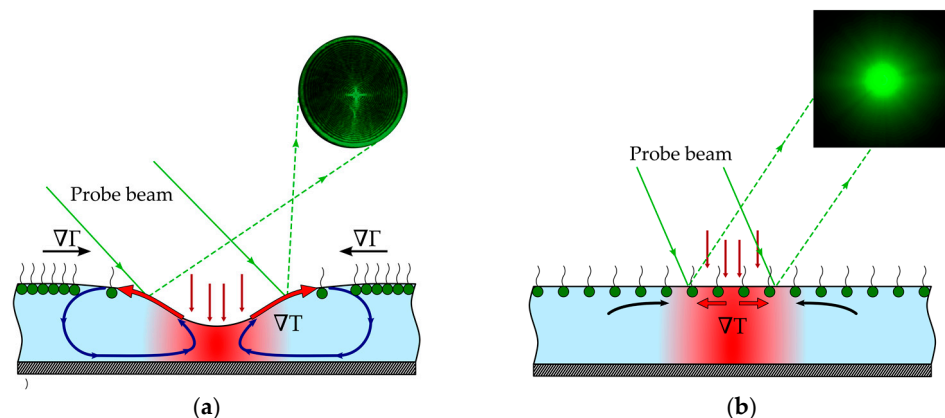


Figure 4. Schematic of the laser-induced thermocapillary convection in a layer with surfactants on the liquid–air interface. (a) The competition between interfacial forces caused by thermal gradient and interfacial forces caused by surfactant concentration gradient (the concentration-driven Marangoni flows); (b) an increase of surface concentration of surfactant molecules suppresses the laser-induced thermocapillary flows and interfacial deformation. This leads to disappearing the PTC signal on a screen.

Using the thermal lens and the probe beam deflection methods [22], it was shown that laser-induced thermocapillary convection in layers of highly light-absorbing liquids (the dyed ethylene glycol and water) was sharply suppressed when adding surfactants (hexadecanol, dipalmitoyl phosphatidylcholine and cardiolipin) in an amount sufficient to reduce interfacial tension by ~ 0.5 mN/m. Thus, one can say that such decrease in interfacial tension is sufficient to suppress the thermal interfacial gradient. The authors noted that the moment, when the thermocapillary deflection is disappeared, corresponds to the gas–liquid-expanded phase transition of the monolayers and can be used as a diagnostic tool.

The effect of the delay of the PTC signal from a thin layer of optically transparent water on the light-absorbing ebonite substrate was found to be very sensitive to presence of any organic impurities on water–air interface [14]. The authors shown that by adding to pure water layer of microdroplets of the solution of hexadecanol in chloroform, the deviation from the quadratic dependence of the delay time is observed. The method enables detection of surface concentrations of $0.3 \mu\text{M}/\text{m}^2$ of hexadecanol in highly purified water.

The generation of thermocapillary vortex flow in a quasi-2D Langmuir monolayer at the liquid–gas interface under irradiating by an IR laser beam was proposed to create a non-contact microfluidic mixer [23].

In [24] it was reported that the thermocapillary convection caused by a heating with a laser beam ($\lambda = 1457$ nm, $P = 15$ mW, the beam spot area is $100 \mu\text{m}^2$) of nanodroplets of aqueous solutions of surfactants and lipids, immersed in dodecanol led to the motion of droplets towards the beam impact area and the formation of stable aggregates. The stability is supported by the formation of lipid bilayers at the contact area between interacting droplets. It is interesting to note that the motion of that droplets was ultimately due to the concentration Marangoni mechanism, caused by the thermocapillary flow inside droplets. This approach provides an opportunity to develop a tool for digital microfluidics and for study thin film drainage and interface stability in emulsion, as well as creating a lipid-bilayer network.

It is interesting to note that the competition between the laser-induced thermocapillary forces at the water–air interface covered with surfactant molecules and the concentration-induced forces, turned out to be the cause of the ambiguity of the measuring data and

a sudden rising the signal when study the interfacial molecules by the sum-frequency generation (SFG) spectroscopy depending on concentration [74]. It was revealed in [75] that high-power IR laser pulses used in the SFG spectroscopy cause the heating of the liquid phase. According to the authors' estimates [75], the temperature increase in a pulse time in the area of the laser beam projection in resonance with OH vibration reaches $\Delta T \approx 19$ K. This temperature gradient induces interfacial flows which transfer molecules away from the area of laser beam in the case of a low concentration of surfactants at the interface. As a result, the signal disappears. Increasing the surfactant concentration creates a strong opposite directed concentration surface tension gradient, which inhibits thermocapillary flows and fills with a dense surfactant monolayer of the irradiated area. This results in the sudden increase in the SFG signal.

Recently, a number of theoretical, numerical, and experimental studies [73,76–78] have been performed to understand the mechanism of influence of surfactant adsorbed at the liquid–air interface on the nature of the thermocapillary flows.

The study [76] reports the results of an experimental and numerical investigation of the influence of an insoluble oleic acid surfactant added to the water–air interface on the development of axisymmetrical thermocapillary flow in the water layer of 7.5 mm thick. The thermocapillary flow was induced by heating of the water with the IR laser beam ($\lambda = 1455$ nm, $2w_0 = 1.26$ mm, $P = 40$ mW). It was shown that the generation of concentration flows caused by the nanoliter addition of surfactants narrows the area of the thermocapillary vortex. These results are consistent with results of a theoretical analysis [77], which show that in the case of convective mass transfer, the front of the thermocapillary flow changes in inverse proportion to the elasticity number characterizing the surfactant film. At the border of the front, both axisymmetric thermocapillary and concentration-capillary flows completely extinguish each other, creating a stagnation zone.

In [78], the instability of thermocapillary flow caused by a laser-heated microbead partially wetting at the water–air interface experimentally investigated. The light-absorbing bead of 300 μm in diameter was glued to an optical fiber through which the laser radiation ($\lambda = 532$ nm) was guided. The power was varied from a few to tens of mW. It was found that an increase in the laser power up to a critical value destroys the axisymmetric structure of the thermocapillary flow and generates dipole and quadrupole vortex flows with opposite directions of rotation. The authors suggested that such instability arises from the inevitable presence of surfactant impurities on the water–air interface. Surfactant molecules are swept away from the heating spot and accumulate near the walls. The surfactant film then creates concentration counter-flows into the heating spot resulting in the azimuthal instability.

3. Laser-Controlled the Liquid–Liquid Interfaces in Multilayer Systems

Thermocapillary flows and instabilities of interfaces in multilayer systems confined between uniformly heated solid surfaces is of great importance in natural and industrial processes [79]. The light-induced convection in the bilayer (the two-layer) liquid systems with a free upper interface is of interest in the development of image recording systems [35–38], nonlinear optics [39,40] and multifunctional optical systems [34].

In [35,36] perturbations of the interface between layers of partially miscible liquids when irradiated by a spatially modulated intensity of an IR laser beam were experimentally and theoretically investigated. Radiation is absorbed in a thin sublayer of the upper layer and produces the thermocapillary stresses on the liquid–air interface. It is shown that in the irradiated parts due to thermocapillary stresses, the free interface deflected, and the liquid–liquid interface acquired a convex shape caused by entrainment with ascending flows in the upper layer (Figure 5). This mechanism was applied by the authors to create a prototype of a highly sensitive IR visible image converter [36–38]. The authors obtained thermal images of real objects [36–38] in the bilayer system with a resolution of 10 lines per mm [38].

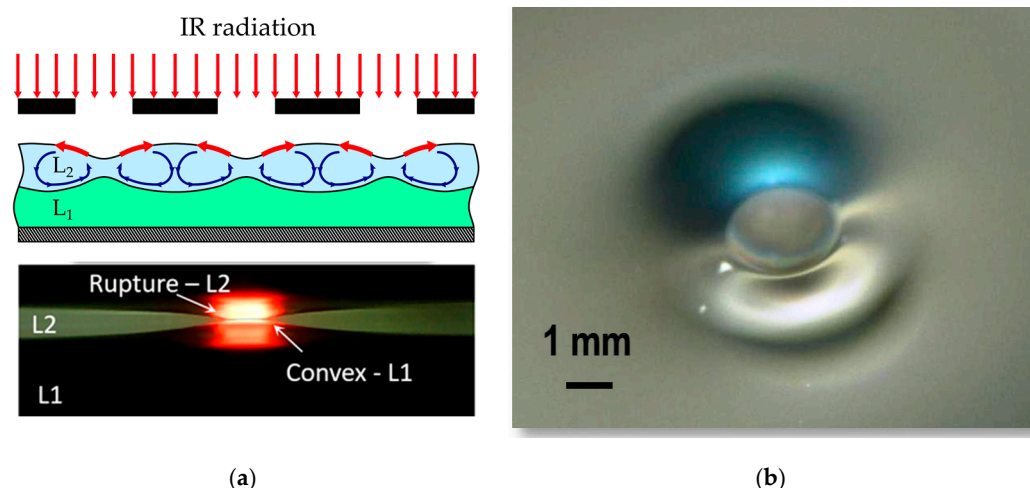


Figure 5. The light-induced thermocapillary effect in bilayer systems with a free liquid–air interface of an upper layer. (a) Illustration of interfacial deformations generated by a spatially modulated radiation in the light-absorbing upper layer (at the top). A side-view not to scale image of the thermocapillary deformation of the liquid–liquid (L1–L2) interface and the rupture of the upper layer caused by a single laser beam according to experimental conditions in [34] (at the bottom); (b) a top-view of the thermocapillary rupture of the bilayer system.

Using a two-layer system as a nonlinear optical medium, the dynamic recording of diffraction gratings of a laser beam were demonstrated [39,40]. A 2–3 μm thick layer of solution of magnetic particles in kerosene imposed on a 1-mm thick layer of water was used in experiments. The modulation of the surface profile was performed due to thermocapillary mass transfer caused by heating with the pump laser beam ($\lambda = 514.5 \text{ nm}$, $P = 140 \text{ mW}$) of the light-absorbing upper layer of the viscous liquid. The results showed that the following factors contribute for improving the diffraction efficiency: an increase in the viscosity of the upper liquid, a decrease in the upper layer thickness, and the use of a liquid layer as a substrate.

In the study [34] an adaptive liquid diaphragm driven by the pumping laser beam was demonstrated. The actuation mechanism is based on the generation of the local thermocapillary circular rupture of the upper layer, which serves as a shutter for passing light. It was shown that the rupture diameter and the focal length of the convex deformation of the bottom layer are varied with the thickness of the upper layer. The bottom layer (glycerol dyed with brilliant green, 2 mm thick) absorbs the pump laser radiation ($\lambda = 632 \text{ nm}$, $P = 17 \text{ mW}$, $2w_0 = 1.5 \text{ mm}$) and creates a heat source at the liquid–liquid interface. Hexadecane dyed with Oil Red O to absorb the passing light ($\lambda = 532 \text{ nm}$, the beam diameter around 50 mm) was used as the upper layer. The aperture diameter increases from 1 to 11 mm when the thickness decreases from 600 to 300 μm . It was observed that a convex deformation of the lower layer operates as a focusing lens with the focal length range from 4 to 25 cm.

In [80,81] the thermocapillary convection in the two-layer system as described in [34] was studied experimentally and theoretically depending on the thickness of the upper and bottom layers. Using the method of scanning laser knife [61] it is shown that the depth of the thermocapillary cavity of the upper layer increases with a decrease in its thickness, similarly to the case of a single-layer systems [61]. Additionally, even in a very thick upper layer, a cavity about 5 μm deep was detected. Measurement of the profile in the rupture area made it possible to find that the height of the convex deformation of the lower layer rises with a decrease in the thickness of the upper one, but does not depend on the thickness of the lower layer in the range of 1–5 mm. A mathematical model [81] is based on the Boussinesq approximation of the Navier–Stokes equations with an intense thermal exposure on the free surface by the laser beam. The model allows one to describe the convex

thermocapillary deformation of the liquid–liquid interface, the thermocapillary concave deflection of the liquid–air interface and predict the rupture time of the upper layer.

The mathematical model of the laser-induced thermocapillary convection in the bilayer and three-layer liquid systems with a closed geometry and anomalous temperature interfacial tension coefficient at the liquid–liquid interface was proposed in [82]. The effect of the ratios of layer thicknesses and liquid viscosities on the amplitude and direction of interface deformations was studied analytically. In the limiting case of equality of viscosities and thicknesses, no deformation in the interfaces was found. Interestingly, despite the simplicity of the model, it appears to be an interesting method to explain and predict the features taking place in optofluidic experiments on droplet dispensing in microchannels [83].

In [84], the modulation of interfacial shapes of a multilayer system under a localized thermal load at the free surface of the upper layer was studied theoretically and numerically. From the numerical study, it was concluded that the convective flows in the layers and the position and shape of the interfaces are determined by the parameters of the system and the properties of the liquids.

4. Conclusions

The phenomena of light-induced thermocapillary convection and the spatial modulation of the interfacial shapes have attracted researchers for a long time as a universal method for solving a wide range of applied problems in microelectronics (the cleaning of silicon wafers, high-resolution lithography), biology (the manipulation of molecules, bacteria, lipid vesicles), the non-contact methods for the testing of liquids and solids, and so on. The advantages of using the thermal action of optical radiation are the following: the delivery of thermal energy to the required place instantaneously and practically lossless; low operating radiation power at the limits of mW; the localization of thermal perturbations on scales smaller than a few micrometers; ensuring the absorption of radiation in the bulk medium or at interfaces; the fast tunability of the power, the radiation flux density and the spatiotemporal distribution of radiation intensity; wavelength choosing for thermal excitation from the IR range (1.4–10.6 μm) absorbed by water or a substrate to the visible range (488–633 nm), which is absorbed by a substrate or dye pigments added to the liquid.

Analysis of the studies shows that a free liquid–air interface, even as a micron-sized air gap between a textured hydrophobic substrate and a liquid, is a necessary condition for generating thermocapillary flows, regardless of the mode of radiation supply.

It is important to note that the laser-induced thermocapillary effect is not limited to problems involving the study of interfacial flows and interface deformation in single- or multilayer systems, as discussed in this review. A large research area is associated with the application of the laser-induced thermocapillary transfer of micro- and nanoobjects suspended in liquid layers/droplets with the free liquid–air interface [1,85,86] or in the confined liquid medium [87–89] for applications in photothermal self-assembly technologies. Interestingly, to generate flows in the confined liquid medium, the free interface activating the motion is artificially created via generating a vapor microbubble on a substrate by heating with a laser beam [87–89]. Moreover, a sharp increase in temperature can be induced by strong radiation absorption of a substrate itself or by the absorption of a plasmonic particle. Such a small area of the liquid–vapor interface is sufficient to create thermocapillary flows that transfer suspended particles to the heated spot.

Funding: This work was funded by the Ministry of Science and Higher Education of the Russian Federation grant number FEWZ-2020-0004.

Institutional Review Board Statement: Not applicable.

Informed Consent Statement: Not applicable.

Data Availability Statement: Not applicable.

Acknowledgments: The author thanks D. Klyuev and V. Fliagin for their technical help.

Conflicts of Interest: The author declares no conflict of interest.

References

1. Li, B.-W.; Zhong, M.-C.; Ji, F. Laser Induced Aggregation of light absorbing particles by Marangoni convection. *Appl. Sci.* **2020**, *10*, 7795. [[CrossRef](#)]
2. Paven, M.; Mayama, H.; Sekido, T.; Butt, H.-J.; Nakamura, Y.; Fujii, S. Light-driven delivery and release of materials using liquid marbles. *Adv. Funct. Mater.* **2016**, *26*, 3199–3206. [[CrossRef](#)]
3. Gao, D.; Ding, W.; Nieto-Vesperinas, M.; Ding, X.; Rahman, M.; Zhang, T.; Lim, C.T.; Qiu, C.-W. Optical manipulation from the microscale to the nanoscale: Fundamentals, advances and prospects. *Light Sci. Appl.* **2017**, *6*, e17039. [[CrossRef](#)] [[PubMed](#)]
4. Hayashi, K.; Yamamoto, Y.; Tamura, M.; Tokonami, S.; Iida, T. Damage-free light-induced assembly of intestinal bacteria with a bubble-mimetic substrate. *Commun. Biol.* **2021**, *4*, 385. [[CrossRef](#)]
5. Da Costa, G.; Calatroni, J. Transient deformation of liquid surfaces by laser-induced thermocapillarity. *Appl. Opt.* **1979**, *18*, 233–235. [[CrossRef](#)]
6. Da Costa, G.; Calatroni, J. Self-holograms of laser-induced surface depressions in heavy hydrocarbons. *Appl. Opt.* **1978**, *17*, 2381–2385. [[CrossRef](#)]
7. Da Costa, G.; Calatroni, J. Interferometric determination of the surface profile of a liquid heated by a laser beam. *Opt. Commun.* **1982**, *42*, 5–9.
8. Da Costa, G.; Escalona, R. Focal properties of liquid films deformed by heating with a Gaussian laser beam. *Opt. Commun.* **1989**, *73*, 1–6. [[CrossRef](#)]
9. Da Costa, G.; Escalona, R. Time evolution of the caustics of a laser heated liquid film. *Appl. Opt.* **1990**, *29*, 1023–1033. [[CrossRef](#)]
10. Bezuglyi, B.A.; Tarasov, O.A. Sensitivity of the thermocapillary method of thickness determination for transparent liquid films on horizontal absorbing substrates. *Tech. Phys. Lett.* **2004**, *30*, 138–140. [[CrossRef](#)]
11. Bezuglyi, B.A.; Tarasov, O.A.; Chemodanov, S.I. Method of Contactless Measuring of Liquid Viscosity. Patent RF 2305271, BI 24 27 August 2007.
12. Bezuglyi, B.A.; Tarasov, O.A.; Fedorets, A.A. Modified tilting-plate method for measuring contact angles. *Colloid J.* **2001**, *63*, 668–674. [[CrossRef](#)]
13. Bezuglyi, B.A.; Chemodanov, S.I. Effect of delay of the thermocapillary response of a transparent liquid layer during laser heating of the absorbing substrate. *Tech. Phys.* **2005**, *50*, 1243–1245. [[CrossRef](#)]
14. Bezuglyi, B.A.; Chemodanov, S.I.; Tarasov, O.A. New approach to diagnostics of organic impurities in water. *Colloid Surf. A* **2004**, *239*, 11–17. [[CrossRef](#)]
15. Tarasov, O.A. Evaluation of the possibility of using the laser-induced thermocapillary effect for photothermal spectroscopy. *Opt. Spectrosc.* **2005**, *99*, 968–974. [[CrossRef](#)]
16. Bezuglyi, B.A.; Zykov, A.Y.; Semenov, S.V. Photothermocapillary diagnostics of near-surface flaws in a solid under a varnish-and paint coating. *Russ. J. Nondestruct. Test.* **2008**, *44*, 391–394. [[CrossRef](#)]
17. Bezuglyi, B.A.; Zykov, A.Y.; Semenov, S.V. Photothermocapillary method for detecting foreign inclusions in solids under paint and varnish coatings. *Tech. Phys. Lett.* **2008**, *34*, 743–746. [[CrossRef](#)]
18. Bezuglyi, B.A.; Zykov, A.Y. Photothermocapillary method for detecting delamination of paint and varnish coatings. *Tech. Phys. Lett.* **2009**, *35*, 650–652. [[CrossRef](#)]
19. Zykov, A.Y.; Ivanova, N.A. Photothermocapillary detection of conductive track ruptures on a printed circuit board coated with a protective film. *J. Phys. Conf. Ser.* **2019**, *1421*, 12039. [[CrossRef](#)]
20. Zykov, A.Y.; Ivanova, N.A. Laser-induced thermocapillary convection in thin liquid layers: Effect of thermal conductivity of substrates. *Appl. Phys. B* **2017**, *123*, 235. [[CrossRef](#)]
21. Khattari, Z.; Hatta, E.; Heinig, P.; Steffen, P.; Fischer, T.M.; Bruinsma, R. Cavitation of Langmuir monolayers. *Phys. Rev. E* **2002**, *65*, 41603. [[CrossRef](#)]
22. Gugliotti, M.; Baptista, M.S.; Politi, M.J. Laser-induced Marangoni Convection in the presence of surfactants monolayers. *Langmuir* **2002**, *18*, 9792–9798. [[CrossRef](#)]
23. Muruganathan, R.; Zhang, Y.; Fischer, T.M. Interfacial thermocapillary vortical flow for microfluidic mixing. *J. Am. Chem. Soc.* **2006**, *128*, 3474–3475. [[CrossRef](#)] [[PubMed](#)]
24. Dixit, S.S.; Kim, H.; Vasilyev, A.; Eid, A.; Faris, G.W. Light-driven formation and rupture of droplet bilayers. *Langmuir* **2010**, *26*, 6193–6200. [[CrossRef](#)] [[PubMed](#)]
25. Wedershoven, H.M.J.M.; Berendsen, C.W.J.; Zeegers, J.C.H.; Darhuber, A.A. Infrared laser induced rupture of thin liquid films on stationary substrates. *Appl. Phys. Lett.* **2014**, *104*, 52101. [[CrossRef](#)]
26. Wedershoven, H.M.J.M.; Berendsen, C.W.J.; Zeegers, J.C.H.; Darhuber, A.A. Infrared-laser-induced thermocapillary deformation and destabilization of thin liquid films on moving substrates. *Phys. Rev. Appl.* **2015**, *3*, 24005. [[CrossRef](#)]
27. van den Temple, M.A.; Wedershoven, H.M.J.M.; Zeegers, J.C.H.; Riepen, M.; Darhuber, A.A. Enhancement of contact line mobility by means of infrared laser illumination. I. Experiments. *Appl. Phys. Lett.* **2016**, *119*, 84904. [[CrossRef](#)]
28. Ivanova, N.; Starov, V.M.; Trybala, A.; Flyagin, V.M. Removal of micrometer size particles from surfaces using laser-induced thermocapillary flow: Experimental results. *J. Colloids Interface Sci.* **2016**, *473*, 120–125. [[CrossRef](#)]

29. Kubochkin, N.S.; Tatosov, A.V.; Al-Muzaiqer, M.; Ivanova, N.A. Detachment of particles from surfaces by thermocapillary flows induced by a moving laser beam. *J. Adhes. Sci. Technol.* **2019**, *33*, 1676–1691. [[CrossRef](#)]
30. Du, F.; Felts, J.R.; Xie, X.; Song, J.; Li, Y.; Rosenberger, M.R.; Islam, A.E.; Jin, S.H.; Dunham, S.N.; Zhang, C.; et al. Laser-induced nanoscale thermocapillary flows for purification of aligned arrays of single-walled carbon nanotubes. *ACS Nano* **2014**, *8*, 12641–12649. [[CrossRef](#)]
31. Singer, J.P.; Lin, P.-T.; Kooi, S.T.; Kimerling, L.C.; Michel, J.; Thomas, E.L. Direct-write thermocapillary dewetting of polymer thin films by a laser-induced thermal gradient. *Adv. Mater.* **2013**, *25*, 6100–6105. [[CrossRef](#)]
32. Bezuglyi, B.A.; Tarasov, O.A. Optical properties of a thermocapillary depression. *Opt. Spectrosc.* **2002**, *92*, 609–613. [[CrossRef](#)]
33. Malyuk, A.Y.; Ivanova, N.A. Varifocal liquid lens actuated by laser-induced thermal Marangoni forces. *Appl. Phys. Lett.* **2018**, *112*, 103701. [[CrossRef](#)]
34. Klyuev, D.S.; Fliagin, V.M.; Al-Muzaiqer, M.; Ivanova, N.A. Laser-actuated optofluidic diaphragm capable of optical signal tracking. *Appl. Phys. Lett.* **2019**, *114*, 11602. [[CrossRef](#)]
35. Loulergue, J.C. Deformation of surfaces of a thin liquid film by thermal perturbation. *Thin Solid Film* **1981**, *82*, 61–67. [[CrossRef](#)]
36. Loulergue, J.C.; Manneville, P.; Pomeaut, Y. Interface deflections induced by the Marangoni effect: An application to infrared-visible image conversion. *J. Phys. D Appl. Phys.* **1981**, *14*, 1967–1977. [[CrossRef](#)]
37. Loulergue, J.C.; Levy, Y.; Imbert, C. Thermal imaging system with a two-phase ternary mixture of liquids. *Opt. Commun.* **1983**, *45*, 149–154. [[CrossRef](#)]
38. Loulergue, J.C.; Xu, S.-L. Infrared photography in liquid films by thermocapillary convection. *Int. J. Infrared Millim. Waves* **1986**, *7*, 171–182. [[CrossRef](#)]
39. Viznyuk, S.A.; Pashinin, P.P.; Sukhodolskii, A.T. Recording dynamic diffraction gratings and optical-phase conjugation by light-capillary profiling of thin liquid-films. *Opt. Commun.* **1991**, *85*, 254–260. [[CrossRef](#)]
40. Viznyuk, S.A.; Pashinin, P.P.; Sukhodolskii, A.T. Formation of dynamic diffraction gratings and phase conjugation under conditions of optocapillary profiling of thin liquid layers. *Sov. J. Quantum Electron.* **1991**, *21*, 560. [[CrossRef](#)]
41. Levich, V.G.; Krylov, V.S. Surface-tension-driven phenomena. *Annu. Rev. Fluid Mech.* **1969**, *1*, 293–316. [[CrossRef](#)]
42. Scriven, L.E.; Sternling, C.V. The Marangoni effects. *Nature* **1960**, *187*, 186–188. [[CrossRef](#)]
43. Legros, J.C.; Limbourg-Fontaine, M.C.; Petre, G. Influence of a surface tension minimum as a function of temperature on the Marangoni convection. *Acta Astronaut.* **1984**, *11*, 143–147. [[CrossRef](#)]
44. Villers, D.; Platten, J.K. Temperature dependence of the interfacial tension between water and long-chain alcohols. *J. Phys. Chem.* **1988**, *92*, 4023–4024. [[CrossRef](#)]
45. Myers, D. *Surfactant Science and Technology*, 3rd ed.; John Wiley & Sons: Hoboken, NJ, USA, 2006.
46. Tatosova, K.A.; Malyuk, A.Y.; Ivanova, N.A. Droplet formation caused by laser-induced surface-tension-driven flows in binary liquid mixtures. *Colloids Surf. A Physicochem. Eng. Asp.* **2017**, *521*, 22–29. [[CrossRef](#)]
47. Ivanova, N.A.; Tatosov, A.V.; Bezuglyi, B.A. Laser-induced capillary effect in thin layers of water-alcohol mixtures. *Eur. Phys. J. E. Soft Matter.* **2015**, *38*, 60. [[CrossRef](#)]
48. Vieyra Salas, J.A.; van der Veen, J.M.; Michels, J.J.; Darhuber, A.A. Active Control of evaporative solution deposition by modulated infrared illumination. *J. Phys. Chem. C* **2012**, *116*, 12038–12047. [[CrossRef](#)]
49. Chevallier, E.; Mamane, A.; Stone, H.A.; Tribet, C.; Lequeux, F.; Monteux, C. Pumping-out photo-surfactants from an air–water interface using light. *Soft Matter* **2011**, *7*, 7866. [[CrossRef](#)]
50. Mamane, A.; Chevallier, E.; Olanier, L.; Lequeux, F.; Monteux, C. Optical control of surface forces and instabilities in foam films using photosurfactants. *Soft Matter* **2017**, *13*, 1299–1305. [[CrossRef](#)]
51. Arya, P.; Umlandt, M.; Jelken, J.; Feldmann, D.; Lomadze, N.; Asmolov, E.S.; Vinogradova, O.I.; Santer, S. Light-induced manipulation of passive and active microparticles. *Eur. Phys. J. E* **2021**, *44*, 50. [[CrossRef](#)]
52. Wunenburger, R.; Issenmann, B.; Brasselet, E.; Loussert, C.; Hourtane, V.; Delville, J.-P. Fluid flows driven by light scattering. *J. Fluid Mech.* **2011**, *666*, 273–307. [[CrossRef](#)]
53. Bayazitoglu, Y.; Lam, T.T. Marangoni convection in irradiating fluids. *J. Heat Transf.* **1987**, *109*, 717–721. [[CrossRef](#)]
54. Indeikina, A.E.; Ryazantsev, Y.S.; Shevtsova, V.M. Unsteady thermocapillary convection in a nonuniformly heated fluid layer. *Fluid Dyn.* **1991**, *26*, 331–337. [[CrossRef](#)]
55. Longtin, J.P.; Hijikata, K.; Ogawa, K. Laser-induced surface-tension-driven flows in liquids. *Int. J. Heat Mass Transf.* **1999**, *42*, 85–93. [[CrossRef](#)]
56. Oron, A. Nonlinear dynamics of irradiated thin volatile liquid films. *Phys. Fluids* **2000**, *12*, 29–41. [[CrossRef](#)]
57. Hitt, D.L.; Smith, M.K. Radiation-driven thermocapillary flows in optically thick liquid films. *Phys. Fluids A Fluid Dynam.* **1993**, *5*, 2624–2632. [[CrossRef](#)]
58. Karlov, S.P.; Kazenin, D.A.; Myznikova, B.I.; Wertgeim, I.I. Experimental and numerical study of the Marangoni convection due to localized laser heating. *J. Non-Equilib. Thermodyn.* **2005**, *30*, 283–304.
59. Marchuk, I.V. Thermocapillary deformation of a horizontal liquid layer under flash local surface heating. *J. Eng. Thermophys.* **2015**, *24*, 381–385. [[CrossRef](#)]
60. Marchuk, I.V. Thermocapillary deformation of a thin locally heated horizontal liquid layer. *J. Eng. Thermophys.* **2009**, *18*, 227–237. [[CrossRef](#)]

61. Klyuev, D.S.; Fliagin, V.M.; Semenov, S.V.; Ivanova, N.A. Thermocapillary deformation induced by laser heating of thin liquid layers: Physical and numerical experiments. *Int. J. Heat Mass Transf.* **2021**, *172*, 121020. [[CrossRef](#)]
62. Barakhovskaia, E.V.; Marchuk, I.V.; Fedorets, A.A. Thermocapillary deformation in a locally heated layer of silicone oil. *J. Phys. Conf. Ser.* **2016**, *754*, 32002. [[CrossRef](#)]
63. Mizev, A.I. Experimental investigation of thermocapillary convection induced by a local temperature inhomogeneity near the liquid surface. 2. Radiation-induced source of heat. *J Appl. Mech. Tech.* **2004**, *45*, 699–704. [[CrossRef](#)]
64. Bar-Cohen, A.; Wang, P. Thermal management of on-chip hot spot. *ASME J. Heat Transf.* **2012**, *134*, 51017. [[CrossRef](#)]
65. Zaitsev, D.V.; Kabov, O.A. An experimental modeling of gravity effect on rupture of a locally heated liquid film. *Microgravity Sci. Technol.* **2007**, *XIX*, 174–177. [[CrossRef](#)]
66. Lyulin, Y.V.; Spesivtsev, S.E.; Marchuk, I.V.; Kabov, O.A. Investigation of disruption dynamics of the horizontal liquid layer with spot heating from the substrate side. *Tech. Phys. Lett.* **2015**, *41*, 1034–1037. [[CrossRef](#)]
67. Kabova, Y.O.; Alexeev, A.; Gambaryan-Roisman, T.; Stephan, P. Marangoni-induced deformation and rupture of a liquid film on a heated microstructured wall. *Phys. Fluids* **2006**, *18*, 12104. [[CrossRef](#)]
68. Zaitsev, D.; Kochkin, D.O.; Kabov, O. Dynamics of liquid film rupture under local heating. *Int. J. Heat Mass Transf.* **2022**, *184*, 122376. [[CrossRef](#)]
69. French, R.H.; Tran, H.V. Immersion lithography: Photomask and wafer-level materials. *Annu. Rev. Mater. Res.* **2009**, *39*, 93. [[CrossRef](#)]
70. Winkels, K.G.; Peters, I.R.; Evangelista, F.; Riepen, M.; Daerr, A.; Limat, L.; Snoeijer, J.H. Receding contact lines: From sliding drops to immersion lithography. *Eur. Phys. J. Spec. Top.* **2011**, *192*, 195–205. [[CrossRef](#)]
71. Garnier, N.; Grigoriev, R.O.; Schatz, M.F. Optical manipulation of microscale fluid flow. *Phys. Rev. Lett.* **2003**, *91*, 54501. [[CrossRef](#)]
72. Gao, A.; Butt, H.-J.; Steffen, W.; Schönecker, C. Optical manipulation of liquids by thermal Marangoni flow along the air-water interfaces of a superhydrophobic surface. *Langmuir* **2021**, *37*, 8677–8686. [[CrossRef](#)]
73. Mizev, A.; Shmyrov, A.; Shmyrova, A. On the shear-driven surfactant layer instability. *J. Fluid Mech.* **2022**, *939*, A24. [[CrossRef](#)]
74. Roke, S.; Schins, J.; Müller, M.; Bonn, M. Vibrational spectroscopic investigation of the phase diagram of a biomimetic lipid monolayer. *Phys. Rev. Lett.* **2003**, *90*, 128101. [[CrossRef](#)] [[PubMed](#)]
75. Backus, E.H.G.; Bonn, D.; Cantin, S.; Roke, S.; Bonn, M. Laser-induced displacement of surfactants on the water surface. *J. Phys. Chem. B* **2012**, *116*, 2703–2712. [[CrossRef](#)] [[PubMed](#)]
76. Pinan Basualdo, F.N.; Terrazas Mallea, R.; Scheid, B.; Bolopion, A.; Gauthier, M.; Lambert, P. Effect of insoluble surfactants on a thermocapillary flow. *Phys. Fluids* **2021**, *33*, 72106. [[CrossRef](#)]
77. Bickel, T. Effect of surface-active contaminants on radial thermocapillary flows. *Eur. Phys. J. E* **2019**, *42*, 131. [[CrossRef](#)]
78. Koleski, G.; Vilquin, A.; Loudet, J.-C.; Bickel, T.; Pouligny, B. Azimuthal instability of the radial thermocapillary flow around a hot bead trapped at the water–air interface. *Phys. Fluids* **2020**, *32*, 92108. [[CrossRef](#)]
79. Nepomnyashchy, A.; Simanovskii, I.; Legros, J.C. *Interfacial Convection in Multilayer Systems*, 2nd ed.; Springer: New York, NY, USA, 2017.
80. Bekezhanova, V.B.; Goncharova, O.N.; Ivanova, N.A.; Klyuev, D.S. Instability of a two-layer system with deformable interfaces under laser beam heating. *J. Sib. Fed. Univ. Math. Phys.* **2019**, *12*, 543–550. [[CrossRef](#)]
81. Bekezhanova, V.B.; Fliagin, V.M.; Goncharova, O.N.; Ivanova, N.A.; Klyuev, D.S. Thermocapillary deformations of a two-layer system of liquids under laser beam heating. *Int. J. Multiph. Flow.* **2020**, *132*, 103429. [[CrossRef](#)]
82. Chraïbi, H.; Delville, J.P. Thermocapillary flows and interface deformations produced by localized laser heating on confident environment. *Phys. Fluids* **2012**, *24*, 32102. [[CrossRef](#)]
83. de Saint Vincent, M.R.; Chraïbi, H.; Delville, J.-P. Optical flow focusing: Light-induced destabilization of stable liquid threads. *Phys. Rev. Appl.* **2015**, *4*, 44005. [[CrossRef](#)]
84. Ovcharova, A.S. Multilayer system of films heated from above. *Int. J. Heat Mass Transf.* **2017**, *114*, 992–1000. [[CrossRef](#)]
85. Miyakawa, K.; Adachi, H. Laser-controlled microscale flows near the air-liquid interface of suspension droplets. *Phys. Rev. E* **2008**, *78*, 41407. [[CrossRef](#)] [[PubMed](#)]
86. Gupta, K.; Kolwankar, K.M.; Gore, B.; Dharmadhikari, J.D.; Dharmadhikari, A.K. Laser-driven Marangoni flow and vortex formation in a liquid droplet. *Phys. Fluids* **2020**, *32*, 121701. [[CrossRef](#)]
87. Namura, K.; Nakajima, K.; Kimura, K.; Suzuki, M. Photothermally controlled Marangoni flow around a micro bubble. *Appl. Phys. Lett.* **2015**, *106*, 43101. [[CrossRef](#)]
88. Setoura, K.; Ito, S.; Miyasaka, H. Stationary bubble formation and Marangoni convection induced by CW laser heating of a single gold nanoparticle. *Nanoscale* **2017**, *9*, 719–730. [[CrossRef](#)]
89. Liu, Z.; Lei, J.; Zhang, Y.; Liu, K.; Liu, W.; Zhang, R.; Zhang, Y.; Yang, X.; Zhang, J.; Yang, J.; et al. All-fiber impurity collector based on laser-induced microbubble. *Opt. Commun.* **2019**, *439*, 308–311. [[CrossRef](#)]